

# Cardiac Gating Visualization and Signal Correlations Using Echocardiogram Imaging and Seismocardiogram Signals

Robert Chen<sup>\*1</sup> and Omer Inan<sup>2</sup>

<sup>1</sup>*Wallace H. Coulter Dept. of Biomedical Engineering, College of Computing,  
Georgia Institute of Technology*

<sup>2</sup>*Principal Investigator, School of Electrical and Computer Engineering, Georgia  
Institute of Technology*

April 24, 2014

## Abstract

Cardiac quiescence periods need to be determined effectively in order to efficiently perform cardiac imaging such as CT and echocardiogram. Accurate methods of cardiac synchronization are crucial for detection of these periods. We treated the deviation detection from echocardiogram processing as the gold standard for quiescent period detection. In this study, we report an initial feasibility study for the detection of quiescent periods using a series of seismocardiogram accelerometers attached to the sternum and the apex (point of maximal inflection - PMI), during echocardiogram imaging.

We collected de-identified echocardiogram, seismocardiogram, and electrocardiogram signals for one subject. We synchronized the signals based upon electrocardiogram readings and applied a series of signal processing methods to the seismocardiogram signals. We compared the ensemble averaged signals for displacement, with the ensemble averaged signals for deviation and ECG from the echocardiogram. We filtered the seismocardiogram displacement signals with various moving average methods in search of a correlation with the deviation from the echocardiogram.

We did not come up with a concrete method for transformation of seismocardiogram signals for the detection of quiescent periods. The study confirmed the difficulty involved in cardiac synchronization with seismocardiogram accelerometers.

## 1 Introduction

Various cardiac synchronization (cardiac gating) methods for imaging purposes are in the development phase in labs across the nation including Emory and Georgia Tech. It is important to be able to correlate periods of the imaging for methods like CT angiogram and ultrasound, with parts of the cardiac cycle.

---

<sup>\*</sup>Corresponding author: rchen87@gatech.edu

This allows us to do a couple important things. On one hand, the gating allows us to determine the periods of cardiac quiescence during imaging process. This allows for doctors to limit exposure of radiation to patients by concentrating the imaging during periods of the cardiac cycle in which the heart is in cardiac quiescence. On the other hand, this allows us to understand the physiological processes that correlate with particular parts of the cardiac cycle that are recorded with the electrocardiogram and seismocardiogram signals.

Physiological processes of interest include normal breathing, breath exhale, and valsalva. As of this writing, a quantitative explanation of cardiac quiescence during these physiological conditions has not been published.

We applied various signal processing methods to smooth out the SCG signals. We searched for correlation between SCG displacement signal and ultrasound deviation signal, with the objective of finding a transformation that can be applied to SCG signals for the prediction of quiescent periods under normal breathing as well as other physiological conditions.

## 2 Data

We used one dataset which consists of the following signals: ultrasound, ECG, and SCG. Cardiac ultrasound was performed for a period of 2 minutes. Ultrasound data was collected using two views: apical four chamber, as well as parasternal long axis. Simultaneously, the ECG and SCG signals were recorded. Accelerometers for the SCG measurement were placed on the apex as well as the sternum. This setup was used for data collection under several physiological scenarios: normal breathing, breath hold during expiration, and valsalva maneuver.

## 3 Results - Normal Breathing

### 3.1 Example echo/hardware recordings from exam

Here we show ONE example of echo recording **14-09-19.ecg**, where we looked at ECG/SCG picked up from the hardware device, as well as from the echo. This represents the normal breathing scenario as recorded from the **apical four chamber** (AFC) view on the echocardiogram.

See figure 1, showing ensemble average of ECG, SCG from our hardware.

For all samples shown in this paper, we show the time window starting from time  $t_r - 300ms$  to  $t_r + 700ms$ , where  $t_r$  corresponds to the time of the  $R$  wave in the ECG signal.

### 3.2 deviation

Figure 2, deviation. Figure 3, deviation and ECG from echocardiogram.

Figure 3, deviation and echo ECG.

### 3.3 velocity from SCG

Use **kalm.m**, which is a kallman filter, on the SCG ensemble averages for  $SCG_{st}$  and  $SCG_{PMI}$ . See figures 4 and 5 showing velocity and figure 6 showing posi-

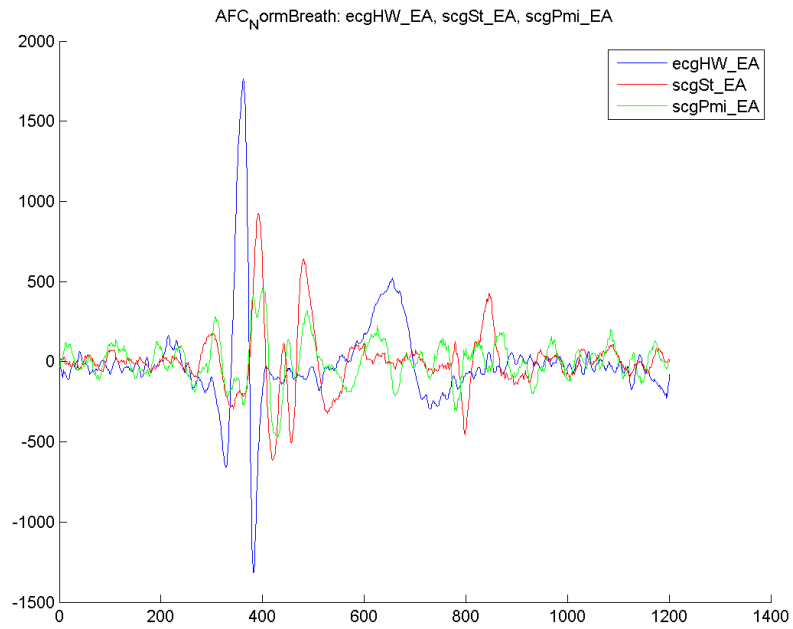


Figure 1: Ensemble average of recordings from hardware: ECG, SCG from sternum, SCG from PMI. **14-09-19.ecg**: AFC view during normal breathing.

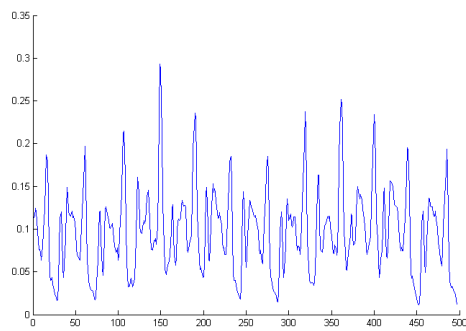


Figure 2: Deviation, exam hardware ECG and echo ECG

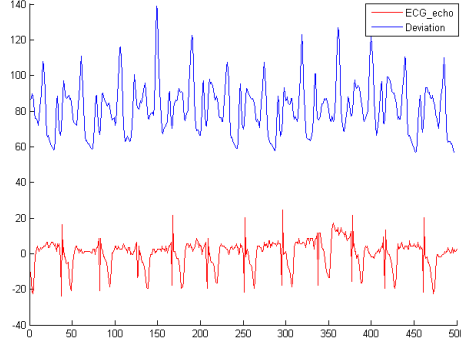


Figure 3: Deviation (blue), ECG from echo (red)

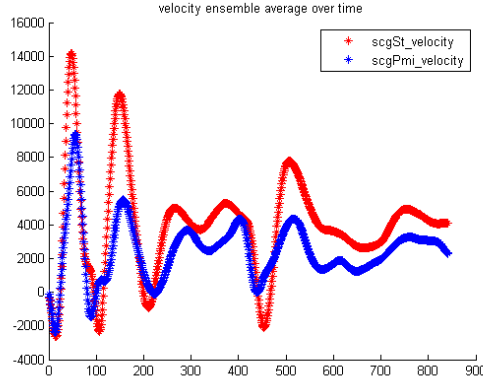


Figure 4: Velocity as recorded from the accelerometers on sternum (red) and PMI (blue).

tion.

In figure 5, we show the velocity from Sternum and PMI SCG signals. For each of these signals  $SCG_{St}$  and  $SCG_{PMI}$ , we found velocities  $\mathbf{v}_{St}$  and  $\mathbf{v}_{PMI}$  using the above method. Next we defined a normalized signal  $\mathbf{v}'_{St} = \mathbf{v}_{St} - \bar{\mathbf{v}}_{St}$  and  $\mathbf{v}'_{PMI} = \mathbf{v}_{PMI} - \bar{\mathbf{v}}_{PMI}$ . Figure 5 shows the plot of the velocity signals obtained.

### 3.4 Position from SCG

#### 3.4.1 Robust determination of position from velocity / acceleration

We used the velocity signal obtained from integration of the  $SCG_{St}$  and  $SCG_{PMI}$  signals. To find the positions  $\mathbf{p}_{St}$  and  $\mathbf{p}_{PMI}$ , we used the cumulative trapezoidal integration of the velocity signals:

$$\mathbf{p}_{St}(t_i) = \int_a^b \mathbf{v}_{St} \approx \frac{h}{2} \sum_{k=i-m}^{i+m} v_{St}(t_{k+1}) + v_{St}(t_k) \quad (1)$$

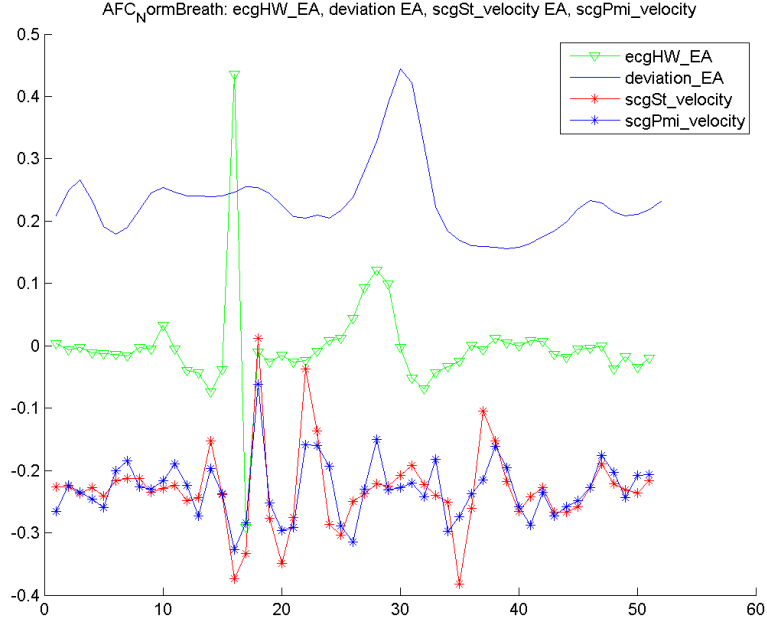


Figure 5: Velocity as recorded from the accelerometers on sternum (red) and PMI (blue). Velocity signal was derived by integrating acceleration signal.

and

$$\mathbf{p}_{PMI}(t_i) = \int_a^b \mathbf{v}_{PMI} \approx \frac{h}{2} \sum_{k=i-m}^{i+m} v_{PMI}(t_{k+1}) + v_{PMI}(t_k) \quad (2)$$

where  $m$  represents the number of samples in each direction from any time point  $p_{St}(t_i)$  or  $p_{PMI}(t_i)$  in order to calculate the trapezoidal integral for that window. For our purpose, we set  $m = 1$ . See figure 6, for plot of the calculated position.

### 3.4.2 Determination of deviation from SCG position

**Absolute Value / SMA** We calculated the "deviations"  $\mathbf{d}_{St}$  and  $\mathbf{d}_{PMI}$  of the SCG signals from the positions  $\mathbf{p}_{St}$  and  $\mathbf{p}_{PMI}$ , using the following process:

$$\mathbf{d}_{St}(t_i) = \frac{1}{m} \sum_{k=i-m}^i |v_{St}(t_k)| \quad (3)$$

and

$$\mathbf{d}_{PMI}(t_i) = \frac{1}{m} \sum_{k=i-m}^i |v_{PMI}(t_k)| \quad (4)$$

. We experimented with various values of  $m$ , varying from  $m = 50$  to  $m = 300$  samples sampled at  $1200Hz$ . We show the calculated deviation for  $m = 50$  in figure 6, for  $m = 100$  in figure 7, and for  $m = 200$  in figure 8.

**SQUARE Value / SMA** We calculated the "deviations"  $\mathbf{d}_{St}$  and  $\mathbf{d}_{PMI}$  of the SCG signals from the positions  $\mathbf{p}_{St}$  and  $\mathbf{p}_{PMI}$ , using the following process:

$$\mathbf{d}_{St}(t_i) = \frac{1}{m} \sum_{k=i-m}^i (v_{St}(t_k))^2 \quad (5)$$

and

$$\mathbf{d}_{PMI}(t_i) = \frac{1}{m} \sum_{k=i-m}^i (v_{PMI}(t_k))^2 \quad (6)$$

. We experimented with various values of  $m$ , varying from  $m = 50$  to  $m = 300$  samples sampled at  $1200Hz$ . We show the calculated deviation for  $m = 50$  in figure 9, for  $m = 100$  in figure 10, and for  $m = 200$  in figure 11.

### 3.4.3 Determination of Quiescent Periods From Calculated SCG Deviation signals

To calculate Quiescent periods based upon SCG deviation signals, we used a cutoff value. See Figures 6, 7, 8, 9, 10, 11 where the threshold value was plotted as a GREEN LINE.

## 4 Discussion

We collected signals from echocardiogram and seismocardiogram during the physiological conditions of normal breathing, exhale, and valsalva. We calculated the deviation of the septum in the echocardiogram during the cardiac cycle and detected quiescent periods based off of this deviation. We filtered the seismocardiogram acceleration signal and used numerical integration methods to obtain the displacement from the acceleration. The displacement signals for the sternum and PMI were obtained via this method.

We applied various signal processing methods to the seismocardiogram acceleration signals we obtained. To obtain the displacement of the sternum and PMI, we performed numerical integration with a method based upon cumulative trapezoidal integration. We smoothed the displacement signal with moving average methods.

We compared ensemble averages for the ECG, echocardiogram deviation, and seismocardiogram displacement signals from the sternum and PMI. We applied a threshold cutoff to the filtered seismocardiogram displacement signals in order to detect quiescent periods. Empirically, we did not see a clear relationship between the seismocardiogram displacement signals and the deviation signals from the echocardiogram.

## 5 Conclusion

We did not find a clear transformation from acceleration signal as obtained from seismocardiogram, to quiescent periods as determined from the deviation signal of the echocardiogram. Our study serves as an initial feasibility study that should motivate future exploration of cardiac gating with seismocardiogram and echocardiogram imaging.

## **6 Acknowledgements**

Thanks to Omer Inan, PhD, Srinidhi Tridandapani, MD, PhD, Carson Wick, PhD for assistance with data collection, materials and guidance on this project.

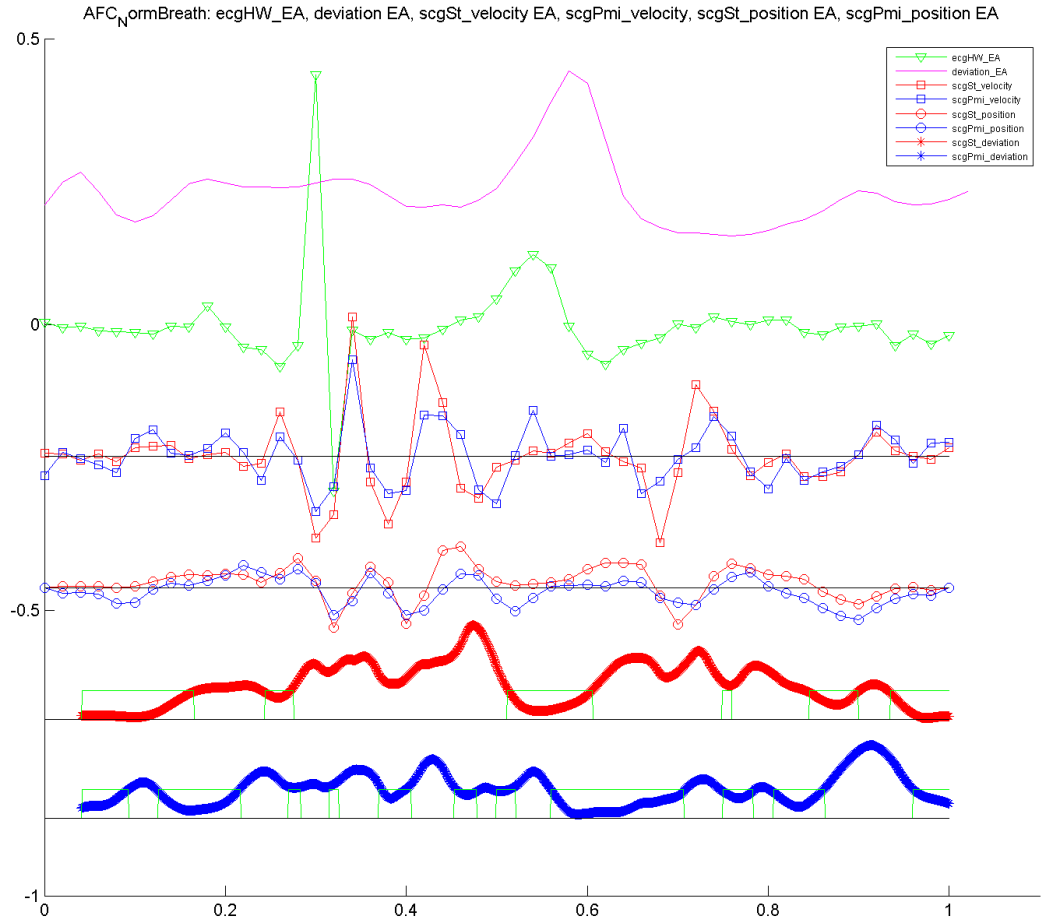


Figure 6: Deviation, ECG, velocity, position, and window average of ABS (position). Absolute value of position was calculated, and a simple moving average of window length 50 frames (@ 1200 Hz) was calculated. Time period for the shown signals is 1 second.



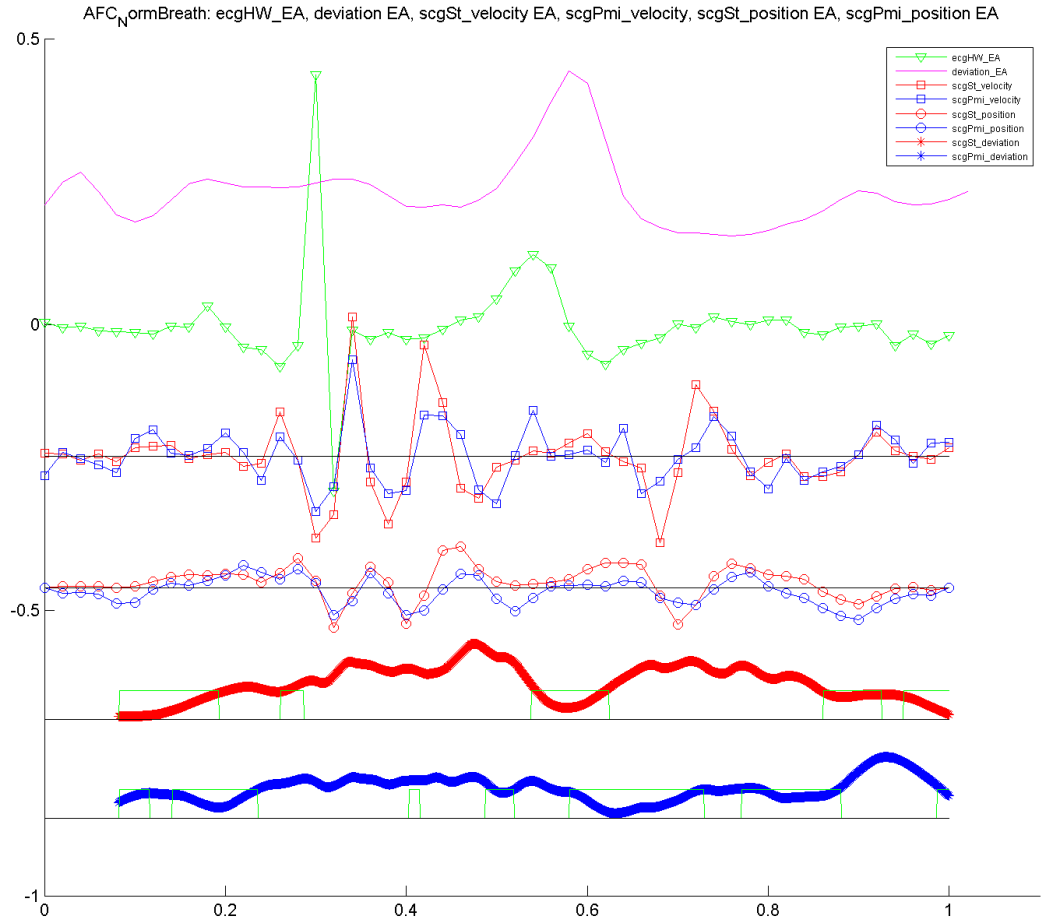


Figure 7: Deviation, ECG, velocity, position, and window average of ABS (position). Absolute value of position was calculated, and a simple moving average of window length 100 frames (@ 1200 Hz) was calculated. Time period for the shown signals is 1 second.

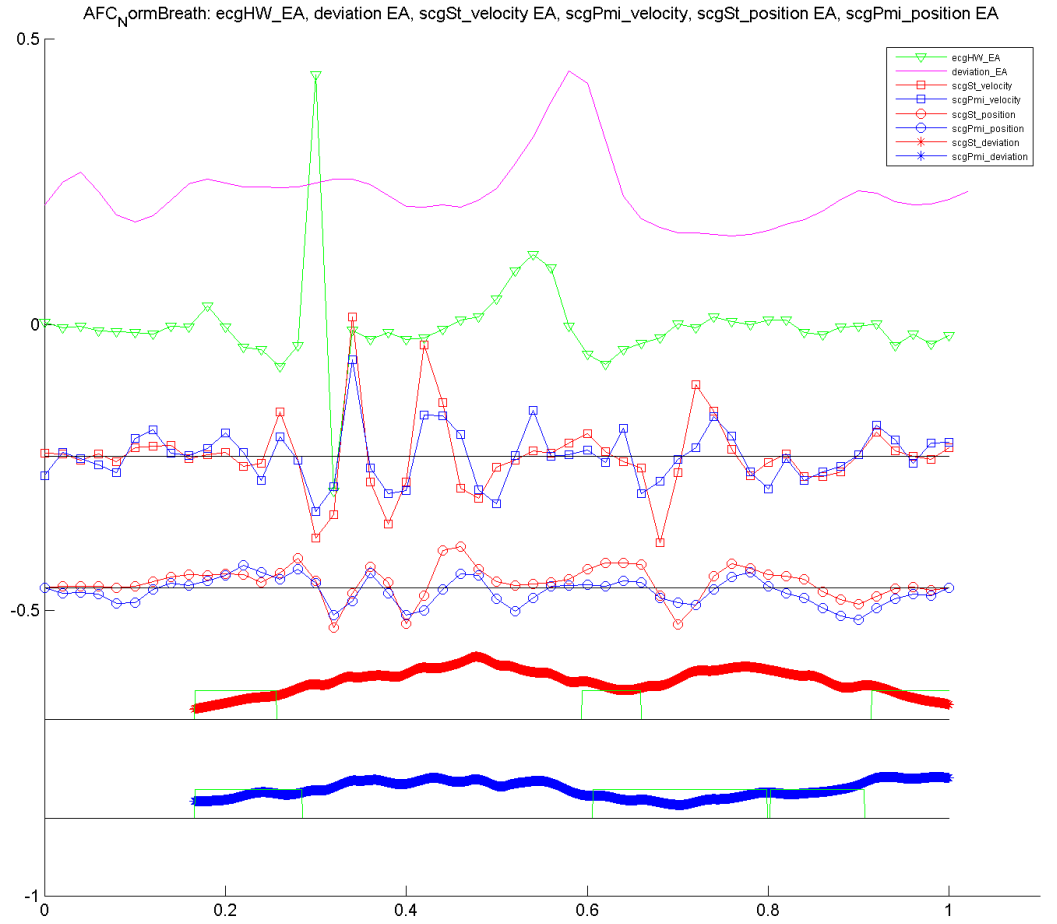


Figure 8: Deviation, ECG, velocity, position, and window average of ABS (position). Absolute value of position was calculated, and a simple moving average of window length 200 frames (@ 1200 Hz) was calculated. Time period for the shown signals is 1 second.

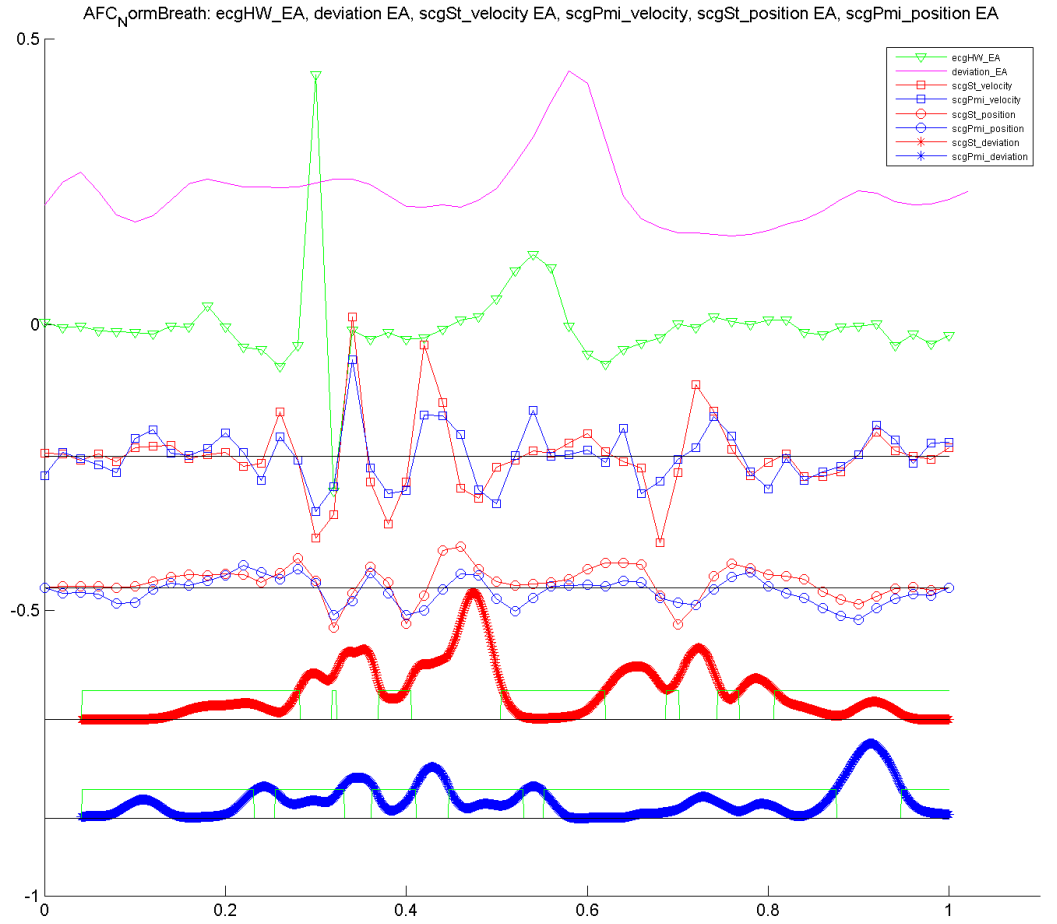


Figure 9: Deviation, ECG, velocity, position, and window average of SQUARED (position). Absolute value of position was calculated, and a simple moving average of window length 50 frames (@ 1200 Hz) was calculated. Time period for the shown signals is 1 second.

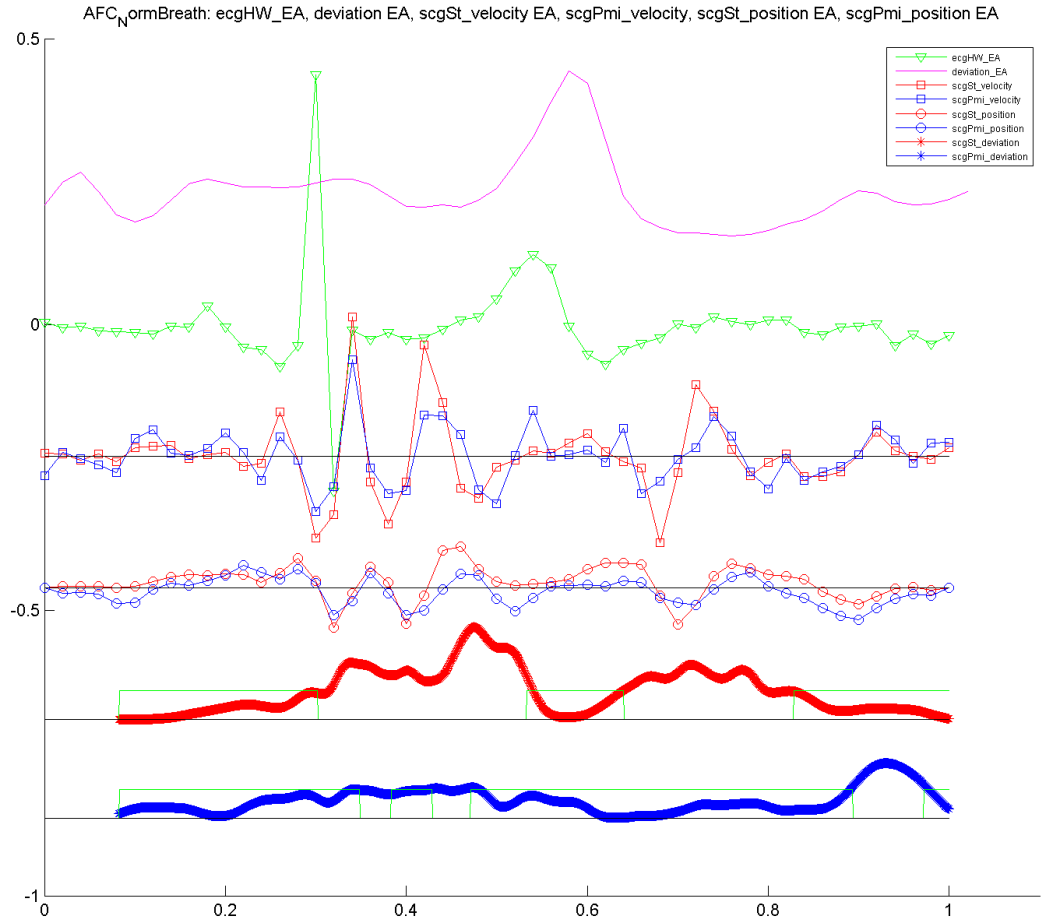


Figure 10: Deviation, ECG, velocity, position, and window average of SQUARED (position). Absolute value of position was calculated, and a simple moving average of window length 100 frames (@ 1200 Hz) was calculated. Time period for the shown signals is 1 second.

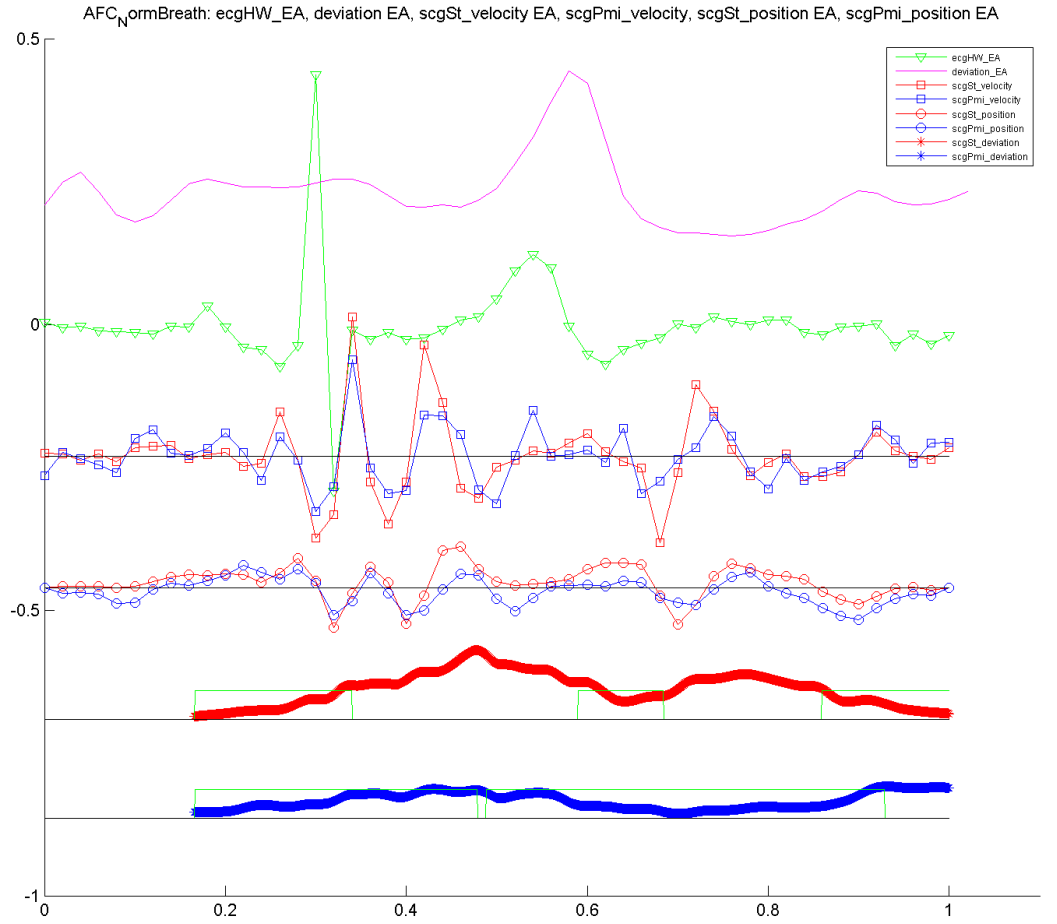


Figure 11: Deviation, ECG, velocity, position, and window average of SQUARED (position). Absolute value of position was calculated, and a simple moving average of window length 200 frames (@ 1200 Hz) was calculated. Time period for the shown signals is 1 second.